Journal of Drug Delivery Science and Technology 53 (2019) 101179

Contents lists available at ScienceDirect

Journal of Drug Delivery Science and Technology

journal homepage: www.elsevier.com/locate/jddst

Hyaluronic acid modified liposomes for targeted delivery of doxorubicin and paclitaxel to CD44 overexpressing tumor cells with improved dual-drugs synergistic effect

Meijia Song[a], Yan Liang[b], Keke Li[a], Jing Zhang[a], Nan Zhang[a], Baocheng Tian[a,*], Jingtian Han[a,**]

[a] School of Pharmacy, Binzhou Medical University, Yantai, PR China
[b] Key Laboratory of Tumor Molecular Biology, Binzhou Medical University, Yantai, PR China

ARTICLE INFO

Keywords:
CD44-Targeting
Hyaluronic acid
pH-sensitive
Combination therapy
Liposome

ABSTRACT

Tumor targeted drug delivery system has been developed as a promising approach to improve cancer chemotherapy. The design of hyaluronic acid (HA)-modified nanocarriers has been proven to be effective for targeting CD44 overexpressing tumor cells. Moreover, combination therapy can improve the therapeutic effect and delay the development of drug resistance. In this study, doxorubicin (DOX) and paclitaxel (PTX) co-loaded liposomal delivery system modified with an acid-cleavable cholesterol-HA conjugate (Chol-HA) was prepared by post-insertion method. The dual-drug co-loaded HA modified liposome (HA-D/P-Lip), had a suitable particle size of 125.5 ± 0.79 nm with negative surface charge of −9.56 ± 0.62 mV, and acceptable encapsulation efficacy of 93.6 ± 0.51% (DOX) and 70.4 ± 1.46% (PTX). *In vitro* drug release study showed that the cumulative release of both drugs over 72 h were much higher in pH 5.5 phosphate buffer than that in pH 7.4 phosphate buffer. *In vitro* cytotoxicity study against MCF-7 breast cancer cells illustrated superior cytotoxicity and obvious synergistic effect in comparison to free drug or single drug loaded liposome via MTT assay. *In vitro* cellular uptake study demonstrated a higher cell internalization of HA-DOX-Lip compared with DOX loaded non-modified liposome (DOX-Lip) and free DOX. Therefore, the pH-sensitive HA-targeted liposome may be a useful targeted nanocarrier for efficient tumor therapy.

1. Introduction

On the basis of WHO data, 8.4 million people die from cancer every year, accounting for nearly 1/6 deaths per year. Cancer is considered as a highly complex disease caused by multiple genetic alterations and constant uncontrolled growth of abnormal cells [1,2]. Chemotherapy has been remained as the mainstream therapy for most of the cancers. There are many kinds of chemotherapeutic agents commonly used in clinic, including doxorubicin (DOX), paclitaxel (PTX), gemcitabine (GEM), vincristine (VCR), docetaxel (DOC) and so forth. DOX is a broad-spectrum anti-tumor antibiotic and has a good effect on many kinds of tumors by interfering with the synthesis of DNA and RNA. However, as the representative drug of anthracycline antibiotics, the main side effect of DOX is cytotoxicity, with cardiac toxicity being the most distinct [3,4]. PTX is a diterpenoid compound extracted from bark of taxus, and it is a new microtubule stabilizer with unique anticancer activity, which is regarded by the National Cancer Institute as the most important progress in cancer chemotherapy in recent 15–20 years. Paclitaxel is limited in clinical use due to resource scarcity and lower water solubility [5~8]. Single use of chemotherapeutic drug in clinical pose enormous practical problems, such as drug resistance, toxic reactions and other severe side effects, and cancer treatment depends on a single antitumor mechanism has become increasingly inappropriate. Combination therapy of two drugs with different antitumor mechanisms to the tumor site for synergistic antitumor effect may be a strategy worth studying, and this combination can not only slow down the development of drug resistance, but also reduce the side effect by decreasing the doses [6,9-13]. The combination of DOX and PTX in clinic is commonly used in the treatment of solid tumors [6]. For instance, Yuan et al. have developed Tf and TAT co-modified liposome delivery system which co-loaded DOX and PTX for the treatment of melanoma, and have showed better therapeutic effect in comparison to single drug loaded liposomes [14]. Lv et al. employed amphiphilic mPEG-b-PLG-b-PLL/DOCA copolymer micelles as carrier to co-loaded DOX and PTX by

* Corresponding author. School of Pharmacy, Binzhou Medical University, 346 Guanhai Road, Yantai, 264003, PR China.
** Corresponding author. School of Pharmacy, Binzhou Medical University, 346 Guanhai Road, Yantai, 264003, PR China.
E-mail addresses: tianzhongmin2001@163.com (B. Tian), hanjingtian002@163.com (J. Han).

https://doi.org/10.1016/j.jddst.2019.101179
Received 22 January 2019; Received in revised form 22 July 2019; Accepted 24 July 2019
Available online 25 July 2019
1773-2247/ © 2019 Elsevier B.V. All rights reserved.

electrostatic adsorption and physical entrapment and obtained a synergistic antitumor effect *in vitro* in A549 cells [15]. Some studies have shown that the combination of DOX and PTX increases tumor regression rates relative to the individual drugs and this combination group has been used as first-line treatment for metastatic breast cancer [16,17].

It is well known that chemotherapeutic drugs have serious side effects, killing tumor cells as well as normal cells, which is due to the low selectivity of the drugs. Nanocarriers, a drug delivery system (DDS) with many excellent properties, is needed to minimize unintended damage came from free drugs. Such as liposome, the artificial biomembrane that is consist of phospholipid bilayer, can be used as a safety carrier for drug delivery by encapsulating the hydrophilic drug in a hydrophilic inner layer or hydrophobic drug in the bilayer [18~21]. Although liposome can accumulate in tumor tissue via enhanced penetration and retention effect (EPR effect), it may be recognized and cleared by reticuloendothelial system (RES) [22~24]. In order to improve this defect, researchers created PEGylated liposomes, which can avoid binding by proteins and removing by RES, thus prolonging the circulation time in blood. However, previous studies showed that PEGylated liposomes hindered interactions between tumor cells and nanocarriers [18]. Researchers in this field have also focused on the active targeting of liposomes via conjugating the ligands on the outer surface of membrane. Hyaluronic acid (HA), is a hydrophilic polysaccharide with negative charge, composed of the repeating D-glucuronic acid and N-acetyl-D-glucosamine linked by β-1, 4 and β-1, 3 glucosidic bonds [51]. HA molecules could specifically bind with CD44 receptors which overexpressed in various tumor cell membrane. Other than that, many researchers indicated that because of its strong hydrophilicity, HA is suitable substitute for PEG. Therefore, HA-modified liposome can not only prolong the drug circulation time, but also increase the affinity of nanocarriers to tumor cells [19,25]. (see Scheme 1)

Tumor microenvironment is very different from normal internal environment in physiological properties. Hypoxia is one of the most prominent signs of tumor microenvironment, and the anaerobic metabolism of tumor cells caused by hypoxia, ultimately lead to the reduction of tumor microenvironment pH. The normal physiological pH value maintains 7.4, however, the pH value in tumor environment is below 6.5. Anti-tumor strategies based on these characteristics of tumor tissues have attracted more and more attention. The pH-sensitive drug release depends on acidic environments in tumor tissue (pH 6.5–7.2), endosome (pH 5.0–6.5) and lysosome (pH 4.5–5.0) in comparison to normal tissue (pH 7.4) [2,26-28]. pH-responsive polymers or nanocarriers have drawn extensively interests in recent years due to their unique environmental sensitive characteristics which can lead to superior therapeutic effect. Wang et al. developed a novel pH/redox dual-responsive polymer which have better controlled drug release profiles and antitumor efficacy *in vitro* [29].

In this study, a cholesterol-butylamine-hyaluronic acid conjugate (Chol-HA) was synthesized. DOX and PTX co-loaded HA-modified liposomes (HA-D/P-Lip) were designed to target the MCF-7 cells with high CD44 receptor expression. A series of related experiments were performed to detect the targeting efficacy and therapeutic effect. Stability study was measured in 50% serum, and drug release study was carried on to compare with non-modified liposomes. Cytotoxicity assays of prepared liposomes were studied in MCF-7 cells. The cellular uptake of HA-D/P-Lip was investigated in comparison to free drug and non-modified liposomes. The endocytosis mechanism of HA-D/P-Lip was explored in MCF-7 cells.

2. Materials and methods

2.1. Materials

Sodium hyaluronate (M_W = 10 kDa) was purchased from Freda biochem Co., Ltd. (Jinan, China). Cholesterol (Chol) and TritonX-100 were supplied by Sigma (USA). Lecithin hydrogenated (HSPC) were supplied by Tywei pharm co., ltd. (Shanghai, China). 4-nitrophenyl

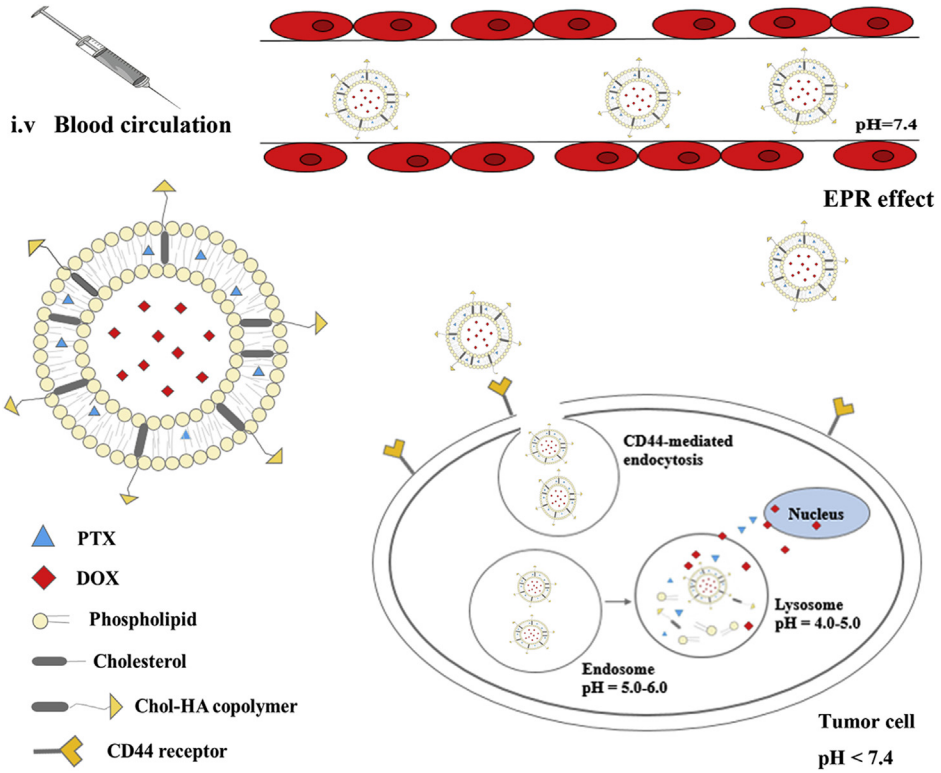

Scheme 1. Basic structure and schematic illustration of DOX and PTX co-loaded HA-modified liposomes (HA-D/P-Lip). HA molecule is a specific ligand for CD44 receptor which expressed on tumor cells. CD44-mediated endocytosis enhanced the cellular uptake of liposomes.

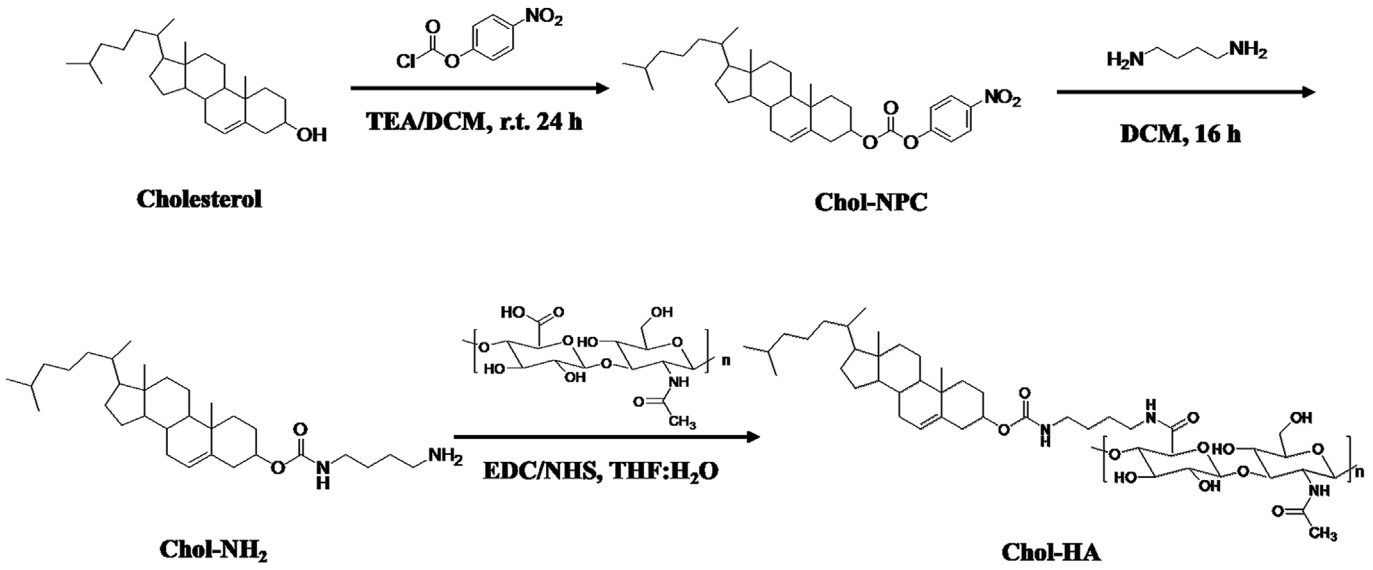

Fig. 1. Synthetic route of Chol-HA copolymer.

chloroformate (4-NPC), 1, 4-butanediamine, 1-Ethyl-3-(3-dimethyl aminopropyl) carbodiimide hydrochloride (EDC·HCl) and N-Hydroxyl succinimide (NHS) were purchased from Aladdin (Shanghai, China). Doxorubicin hydrochloride (DOX·HCl) and paclitaxel (PTX) were purchased from Melone biotech co., ltd. (Dalian, China). 3-(4, 5-dimethylthiazol-2-yl)-2, 5-diphenyltetrazolium bromide (MTT), DAPI and Sepharose CL-4B were purchased from Sigma (USA). Fetal bovine serum (FBS), trypsin-EDTA, RPMI-1640 medium and Dulbecco's modified Eagle's medium (DMEM) were obtained from Hyclone (USA). Methanol, chloroform, dimethyl sulfoxide, acetonitrile, dichloromethane and tetrahydrofuran were purchased from local dealers. All materials were used as received without further purification.

2.2. Synthesis and characterization of Chol-HA conjugate

The cholesterol derivative (Chol-HA conjugate) was prepared by the following three steps. The synthesis route is shown in Fig. 1.

2.2.1. Synthesis of Chol-NPC

Chol-NPC was synthesized based on a modified procedure [30]. The hydroxyl group of cholesterol was activated by 4-NPC. Briefly, cholesterol (1 mmol) was dissolved in anhydrous dichloromethane containing anhydrous triethylamine (2 mmol). Then, 4-NPC (1.2 mmol) was added slowly to the above solution under stirring at 0 °C for 2 h, and the mixture solution was removed from 0 °C to room temperature for another 24 h. The reaction mixture was concentrated by a rotary evaporator, and the resulting product was purified by precipitating in cold methanol. The final white loose solid was dried in vacuo for 48 h, and the yield of Chol-NPC was about 75%.

2.2.2. Synthesis of Chol-NH_2

The introduction of connecting arm was achieved by the reaction of Chol-NPC with 1, 4-butanediamine via ammonolysis reaction [31]. Briefly, a solution of Chol-NPC (150 mg, 0.27 mmol) was added slowly to 15 mL DCM solution containing 1, 4-butanediamine (305 mg, 2.7 mmol) and triethylamine (376 μL) at room temperature. After the reaction was stirred at room temperature for 16 h, the solution was concentrated and precipitated in cold methanol. The final yellowish solid was dried in vacuo for 24 h, and the yield of Chol-NH_2 was about 55%.

2.2.3. Synthesis of Chol-HA

The binding of hyaluronic acid to cholesterol was mediated by acylation reaction [32]. Briefly, HA (100 mg) was dissolved in distilled water, and stirred with EDC and NHS for 1 h to activate the carboxyl group (the molar ratio of –COOH: EDC: NHS is 1:2:5). Then, Chol-NH_2 (107 mg) in THF (12 mL) was added dropwise to the above HA solution under 45 °C. After stirred for 6 h, the reaction mixture was dialyzed in dialysis bag (MWCO 10 kDa) against distilled water/THF (1:1, v/v) solution and distilled water, respectively. We freeze-dried the dialyzed solution and could obtain cholesterol-hyaluronic acid (Chol-HA) conjugate as white floccule with a general yield of 32%.

The chemical structure of Chol-NPC, Chol-NH_2 and Chol-HA were characterized by Fourier transform infrared spectroscopy (FTIR, Antaris, USA) and ^{1}H nuclear magnetic resonance spectrometry (^{1}H NMR, Bruker, Switzerland). The degree of substitution (DS) of cholesterol was defined as the number of cholesterol molecules per 100 sugar residues of HA.

2.2.4. Hemolysis test

The blood compatibility of Chol-HA conjugate was validated by hemolysis test with slight modification [33]. Red blood cells were separated with plasma by centrifugation at 1000 r/min for 10 min, and washed with 0.9% NaCl until the supernatant is colorless. Erythrocytes were diluted to 2% suspension with 0.9% NaCl. In this experiment, 0.9% NaCl was used as negative control solution, 2% TritonX-100 as positive control solution, and Chol-HA conjugate of different concentrations (0.1, 0.2, 0.5, 1, 2 mg/mL) as samples to be tested. 1 mL of RBCs suspension was mixed with 1 mL of the above solutions. The mixture was incubated in a shaker at 37 °C for 2 h and then centrifuged at 1000 r/min for 10 min. The absorbance of the supernatant at 545 nm was measured by UVs (UV-2450, Shimadzu, Japan). Hemolysis percentage was calculated as follows:

$$\text{Hemolysis (\%)} = (A_S\text{-}A_N) / (A_P\text{-}A_N) \times 100,$$

Where A_S, A_P and A_N are the absorbance values of sample, positive control and negative control, respectively.

2.3. Liposome preparation and characterization

The DOX and PTX loaded HA-modified liposomes (HA-D/P-Lip) were prepared by thin-film method, ammonium sulfate gradient method and post-insertion method with mild modification [34~38]. Briefly, PTX, HSPC and cholesterol (HSPC:Chol = 60:35, *n/n*, PTX:total lipids = 1:20, *w/w*) were dissolved in the mixture of methanol and chloroform (*v/v* = 1:3) solution. Then the organic solvent was removed

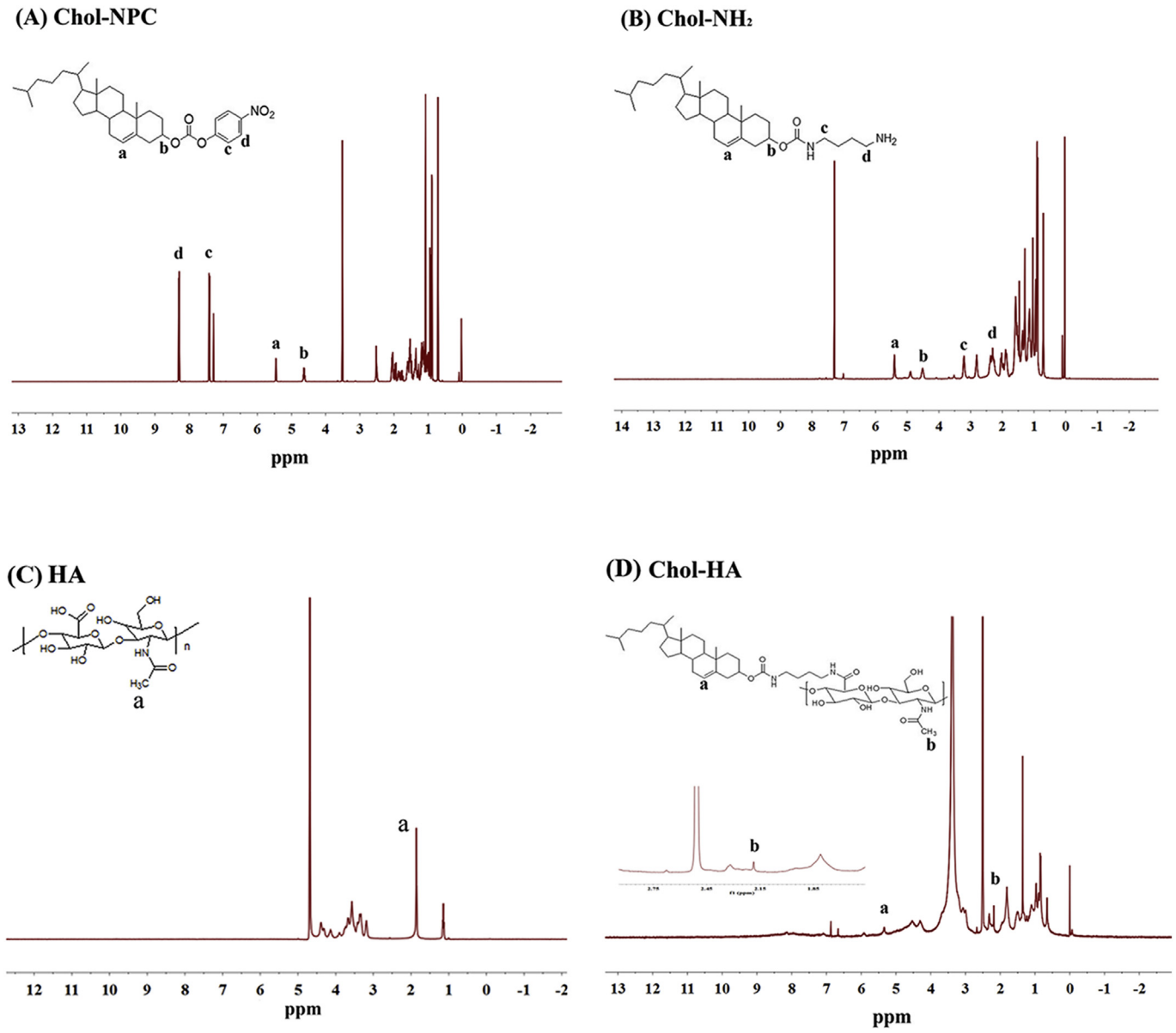

Fig. 2. ^{1}H NMR spectra of Chol-NPC in $CDCl_3$ (A), Chol-NH_2 in $CDCl_3$ (B), HA in D_2O (C) and Chol-HA in DMSO-d_6 (D).

by rotary evaporation and the film was further dried in vacuum overnight. The film was hydrated with 180 mM $(NH_4)_2SO_4$ solution (pH = 4.2) at 47 °C for 1 h. Then, it was sonicated intermittently by a probe sonicator at 200 w for 2 min and 400 w for 2 min in an ice bath to form PTX loaded liposomes (PTX-Lip). Free ammonium sulfate in aqueous phase outside liposomes was exchanged by dialysis method against 5% glucose solution. For the preparation of DOX-loaded liposomes, DOX (doxorubicin hydrochloride:total lipids = 1:10, *w/w*) was dissolved in 1 mL 5% glucose solution, and then incubated with the above liposomes at 50 °C for 15 min under gentle shaking. Free PTX and DOX was removed by centrifugation and dialysis method. HA-modified DOX and PTX co-loaded liposomes were prepared by post-insertion method via embedding the Chol-HA conjugate into lipid bilayer. A certain proportion of Chol-HA conjugate (10 mol% of total lipids) was incubated with the above liposomes for 30 min at 50 °C. Finally, unincorporated Chol-HA conjugate was removed by size-exclusion chromatography with Sepharose CL-4B column.

The free Chol-HA conjugate separated by size-exclusion chromatography was quantitatively determined the content of Chol-HA inserted into liposome bilayers by carbazole method [39,40]. Each sample was performed in triplicate.

The mean particle size, polydispersity index (PDI) and zeta potential of different liposomes were estimated by Malvern Zetasizer nano ZS90 instrument (Malvern, UK). Each sample was determined in triplicate at room temperature.

The morphology of prepared liposome was observed by transmission electron microscopy (TEM, JEM-1230, Japan). Liposomes were dropped on a copper grid and dried on room temperature, and 2% phosphotungstic acid solution was added at least 2 min for negative staining. At the end, samples were observed by TEM.

Fluorescence spectrophotometer (F-2700, Hitachi, Japan) was used to determine the content of DOX (Em = 587 nm, Ex = 497 nm), and the content of PTX was measured by HPLC (Agilent 1260, USA) with the mobile phase of acetonitrile: ultrapure water (60:40, *v/v*) and the detection wavelength is at 227 nm. The encapsulation efficiency (EE %) and drug loading (DL %) were calculated as follows:

$$\text{EE}\ (\%) = \frac{W_A}{W_B} \times 100,$$

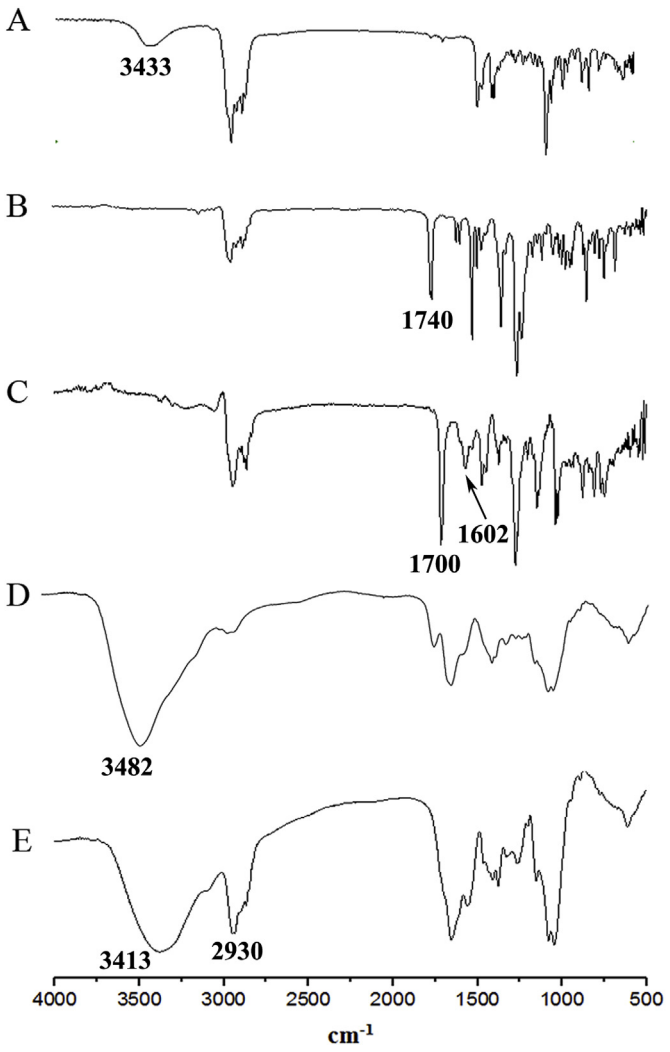

Fig. 3. FTIR spectrum of Chol (A), Chol-NPC (B), Chol-NH2 (C), HA (D) and Chol-HA (E).

Table 1
Hemolysis rate of micelles solutions (mean ± SD, n = 3).

Samples	Concentration (mg/mL)	Hemolysis (%)
0.9% NaCl	/	0
2% TritonX-100	/	100
	0.1	0.79 ± 0.12
	0.2	1.26 ± 0.26
Chol-HA copolymers	0.5	1.83 ± 0.35
	1	2.44 ± 0.71
	2	3.59 ± 0.22

$$\text{DL } (\%) = \frac{W_A}{W_L} \times 100$$

Where, W_A, W_B and W_L representing the amount of drug in liposomes, the initial amount of drug and the total weight of liposome, respectively.

2.4. In vitro stability studies

In order to verify the stability of liposomes during blood circulation, HA-D/P-Lip and D/P-Lip were mixed with 50% FBS and pH 7.4 PBS buffer respectively under shaking at 37 °C. At each predetermined time point, 1 mL of sample was taken out for the particle size measurement by Nano Zetasizer instrument.

2.5. In vitro drug release

The drug release assay was measured using dialysis method under sink conditions at 37 °C in pH 7.4 and pH 5.5 PBS buffer containing 0.2% (w/v) Tween 80 (Yuan et al., 2016). Approximately, a known quantity of liposome and free drug were put in a dialysis bag (4000 Da), sealed and immersed into 40 mL PBS buffer under mild stirring. 5 mL of medium was withdrawn and added with equal volume of fresh medium at each predetermined time point (0.5, 1, 2, 4, 6, 8, 10, 12, 24, 36, 48, 60 and 72 h). The amount of released DOX and PTX was measured using the fluorescence spectrophotometry and HPLC method. Each sample was repeated in triplicate.

2.6. Cell line and cell culture

MCF-7 cells (human breast cancer cells) were relatively high CD44 expression and cultured in RPMI-1640 medium. HepG2 cells (human liver hepatocellular carcinoma cells) were relatively lower CD44 expression and cultured in DMEM medium [33,41]. L929 cells (mouse fibroblast cells) were cultured in RPMI-1640 medium. All cells were grown in a humidified incubator at 37 °C under 5% CO_2 atmosphere supplemented with 10% FBS and 1% antibiotics (streptomycin, 100 μg/mL, penicillin, 100 U/mL). All the cells used in this study were supplied by Shanghai Institute of Cell.

2.7. In vitro cellular uptake

2.7.1. Confocal laser scanning microscopy (CLSM)

Qualitative analysis of cellular uptake was evaluated by CLSM. MCF-7 cells and HepG2 cells were seeded onto round coverslips in 6-well plate at a density of 1×10^5 cells/well and incubated for 24 h to completely adhere. Then the medium was absorbed and discarded. The cells were cultured in medium containing liposomal formulations and free DOX, with the final DOX concentration is 10 μg/mL. Following by incubating for 2 and 4 h, cells were washed with PBS for three times, and fixed with 4% (*w/v*) paraformaldehyde for 30 min at room temperature. Next, the cell nucleus was stained by DAPI solution for 10 min. Finally, the dye was washed and the cells on coverslips were harvested for image acquisition by CLSM (TCS SPE, Leica, Germany).

Table 2
The size, zeta potential and encapsulation efficiency of liposomal formulations (mean ± SD, n = 3).

Samples	Size (nm)	PDI	Zeta potential (mV)	EE (%)-DOX	DL (%)-DOX	EE (%)-PTX	DL (%)-PTX
Blank Lip	94 ± 1.02	0.211 ± 0.03	−1.81 ± 1.02	/		/	
HA-Lip	109 ± 0.55	0.242 ± 0.21	−9.62 ± 1.03	/		/	
D-Lip	94 ± 0.37	0.138 ± 0.02	1.92 ± 0.22	94.6 ± 1.01	9.31 ± 0.58	/	
P-Lip	95 ± 0.12	0.222 ± 0.55	−2.13 ± 0.71	/		75.3 ± 1.04	3.96 ± 0.79
D/P-Lip	96 ± 0.38	0.241 ± 0.17	1.24 ± 0.15	95.1 ± 0.88	9.93 ± 0.50	72.7 ± 0.75	3.48 ± 0.95
HA-D-Lip	121 ± 1.01	0.203 ± 0.15	−10.74 ± 1.18	93.4 ± 0.29	8.01 ± 0.25	/	
HA-P-Lip	117 ± 0.66	0.192 ± 0.02	−9.36 ± 0.78	/		72.2 ± 0.62	3.46 ± 0.17
HA-D/P-Lip	125 ± 0.79	0.212 ± 0.02	−9.56 ± 0.62	93.6 ± 0.51	8.04 ± 1.01	70.4 ± 1.46	3.12 ± 0.81

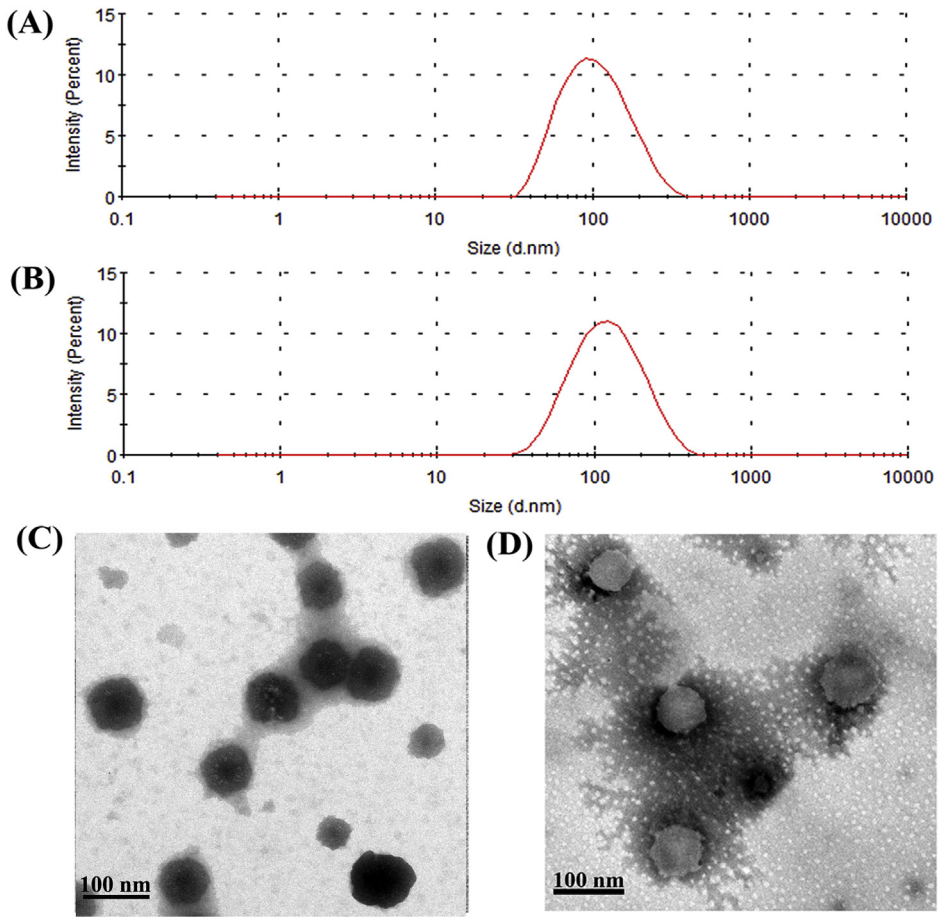

Fig. 4. Size distribution graph of HA-Lip (A) and HA-D/P-Lip (B). The TEM image of HA-D/P-Lip (C) and HA-Lip (D).

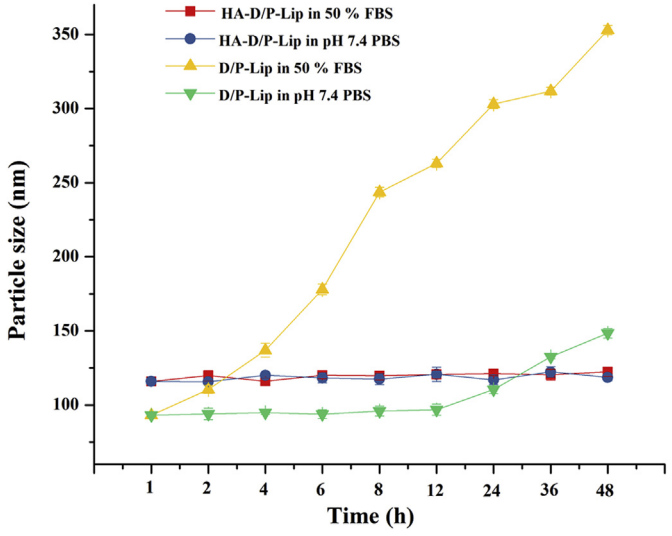

Fig. 5. Stability studies of HA-D/P-Lip and D/P-Lip after incubation in 50% FBS and pH 7.4 PBS at 37 °C for 48 h (mean ± SD, n = 3).

2.7.2. Flow cytometry (FCM)

Quantitative analysis of cellular uptake was estimated by FCM. Briefly, MCF-7 cells and HepG2 cells were seeded onto 6-well plate at a density of 1×10^5 cells/well. The remaining steps were the same as described in 2.7.1. After incubation for 2 and 4 h, cells were washed three times with cold PBS to stop the drug ingestion. Cells were collected by trypsin digestion, centrifuged and re-suspended in 0.5 mL PBS for FCM analysis (EPICS XL, Beckman, USA) with the excitation wavelength at 488 nm and the emission wavelength at 525 nm. 1×10^4 events were analyzed by the FCM software for each sample.

2.8. Identification of uptake pathways

In order to investigate the mechanism of internalization of HA-DOX-Lip, MCF-7 cells were pre-incubated with different inhibitors for 1 h at 37 °C. Amiloride (1.48 mg/mL), chlorpromazine (30 μg/mL), NaN_3 (30 μg/mL), β-CD (1 mg/mL) and free HA (1 mg/mL) were added. The cells were incubated under both 37 °C and 4 °C to detect the influence of temperature on cellular uptake. Then inhibitors were discarded and HA-DOX-Lip was added for another 2 h. The cells were treated as described in 2.7.2.

2.9. Biocompatibility and in vitro antitumor activity

2.9.1. Biocompatibility assay

The biocompatibility of blank liposomes was investigated in MCF-7 cells, HepG2 cells and L929 cells by MTT assay. Briefly, cells were seeded in 96-well plate at a density of 1×10^4 cells/well and then incubated at 37 °C under 5% CO_2 atmosphere overnight. Cells were treated with HA-modified blank liposomes (HA-Lip) to yield varying concentrations from 0.1 to 50 μg/mL (the concentration was calculated as Chol-HA conjugate). After cultured for 48 h, the solution in the plate was discarded, and added 20 μL MTT solution (5 mg/mL) to each well, followed by incubating for another 4 h. Finally, the medium was replaced with 150 μL DMSO and oscillated at 37 °C for 10 min until the crystalline substances were completely dissolved. The absorbance value at 490 nm was recorded by a microplate reader. Data are expressed as

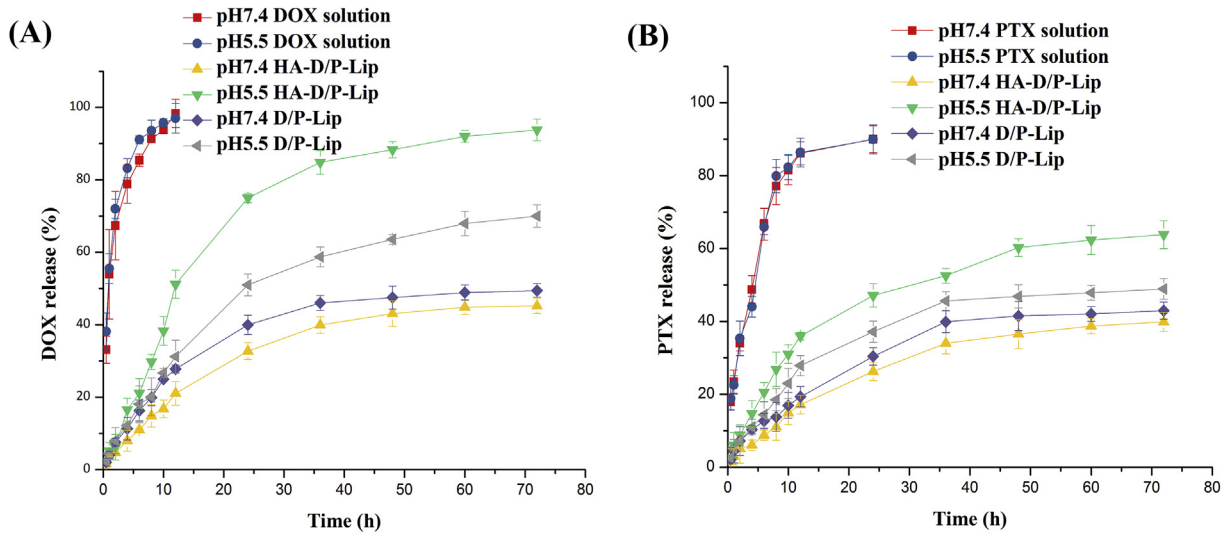

Fig. 6. The DOX (A) and PTX (B) release profiles of liposomal formulations in pH 7.4 and pH 5.5 PBS buffer over 72 h at 37 °C (mean ± SD, n = 3).

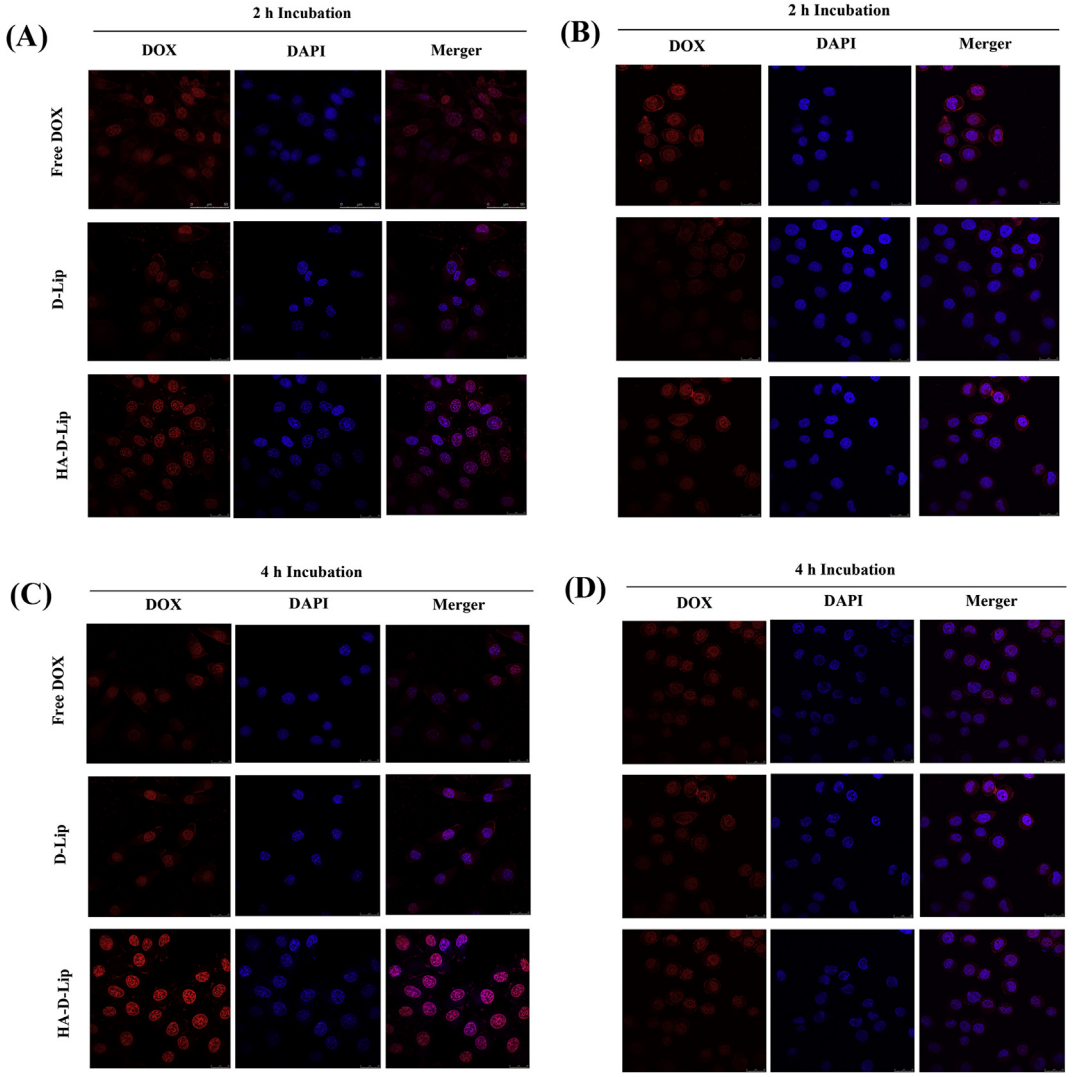

Fig. 7. CLSM images of MCF-7 cells (A) and HepG2 cells (B) after 2 h incubation, MCF-7 cells (C) and HepG2 cells (D) after 4 h incubation with free DOX, D-Lip and HA-D-Lip (equivalent to 10 μg/mL DOX).

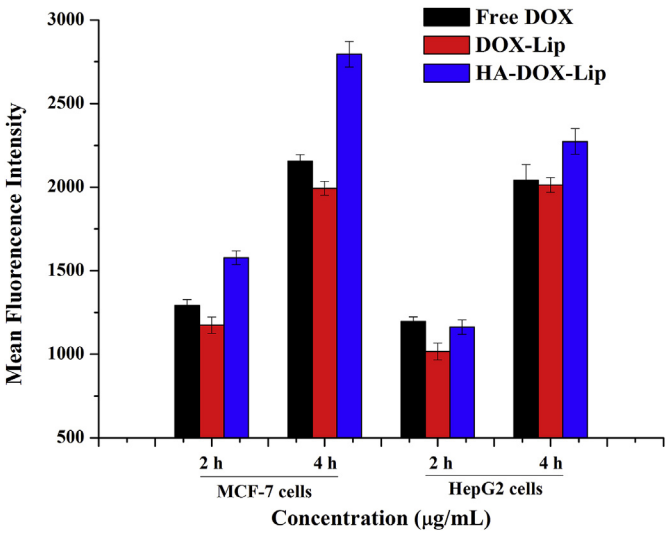

Fig. 8. FCM analysis of 10 μg/mL of free DOX, DOX-Lip and HA-DOX-Lip in MCF-7 and HepG2 cells after incubation for 2 h (A) and 4 h (B).

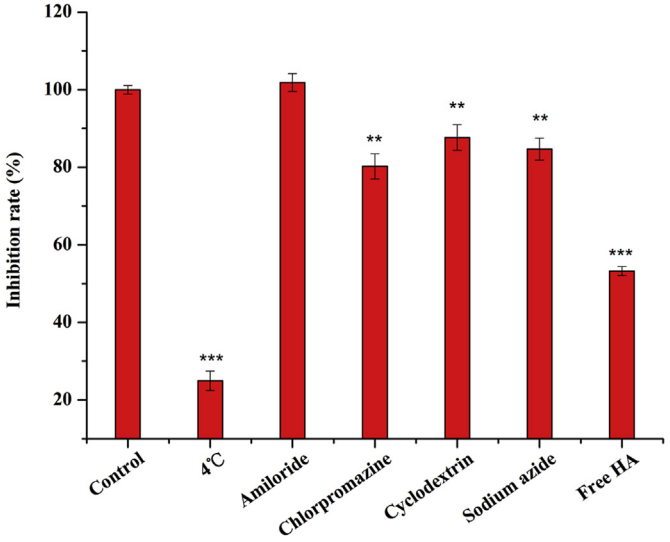

Fig. 9. The endocytosis inhibition study on MCF-7 cells (mean ± SD, n = 3). *** and ** indicate $P < 0.001$ and $P < 0.05$ versus control group.

mean ± standard deviation (n = 6). Cell viability was calculated as follows:

$$\text{Cell viability (\%)} = \text{OD}_{\text{treatment group}}/\text{OD}_{\text{control group}} \times 100$$

2.9.2. In vitro cytotoxicity and synergistic efficacy

The cytotoxicity of free drugs and drug-loaded liposomes against MCF-7 cells was evaluated by MTT assay. MCF-7 cells were seeded in 96-well plate at a density of 1×10^4 cells/well and then incubated at 37 °C under 5% CO_2 atmosphere overnight. The culture medium was replaced with serial concentrations of free drugs or liposome solutions. After cultured for 48 h, the solution in the plate was discarded, and added 20 μL MTT solution (5 mg/mL) to each well, followed by incubating for another 4 h. Finally, the medium was replaced with 150 μL DMSO and oscillated at 37 °C for 10 min until the crystalline substances were completely dissolved. The absorbance value at 490 nm was recorded by a microplate reader. Results are reported as mean ± SD (n = 6). The half inhibitory concentration (IC_{50}) values were calculated using Origin 8.0 software according to the fitting data. The Combination Index (CI_{50}) was measured according to the Chou and Talalay's method [41] [52], and used to distinguish synergistic, additive, or antagonistic cytotoxic effects.

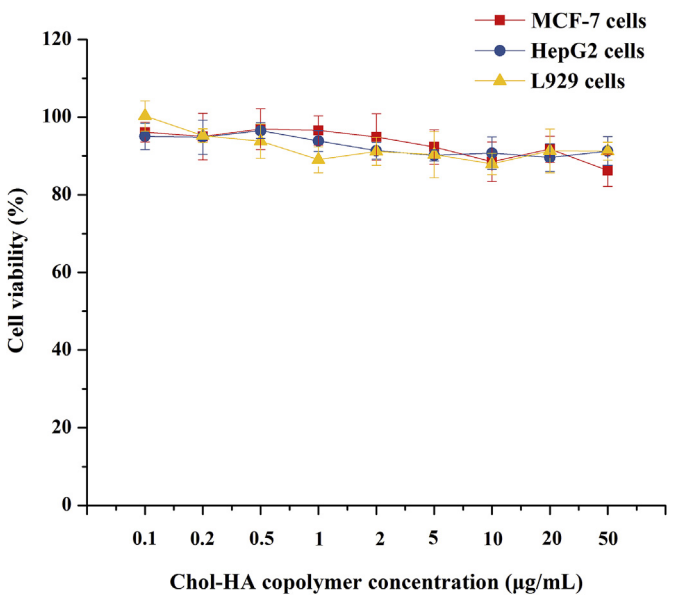

Fig. 10. Biocompatibility assay of HA-Lip (mean ± SD, n = 6).

$$CI_X = \frac{(D)_1}{(D_x)_1} + \frac{(D)_2}{(D_x)_2}$$

Where, $(Dx)_1$ and $(Dx)_2$ representing the IC_{50} value of free drug 1 alone and free drug 2 alone respectively. D_1 and D_2 representing the IC_{50} value of drug 1 and drug 2 in combination system. $CI_{50} > 1$ representing the antagonism of dual-drug combination, $CI_{50} = 1$ representing the additive effect of dual-drug combination and $CI_{50} < 1$ representing the synergistic effect of dual-drug combination.

2.10. Statistical analysis

Data were expressed as mean ± standard deviation (SD). Student's test was used to determine the statistical significances between two groups. $P < 0.05$ was regarded as significant differences.

3. Results and discussion

3.1. Synthesis of Chol-HA conjugate

Amphiphilic Chol-HA conjugate was synthesized by three steps. The structure of reaction products were confirmed by FTIR and ^{1}H NMR.

First step, the terminal hydroxyl group of cholesterol was connected with the active acyl chloride group of NPC to form cholesterol ester by an acylation reaction. As shown in Fig. 2A, the signals at 7.47 ppm and 8.32 ppm were characteristic absorption of aromatic proton (Ar–H). The typical signals of the cholesterol moiety was observed at 5.45 ppm (-CH═C), 4.52 ppm (–CHOCO–). In FTIR spectra of Chol-NPC (Fig. 3, curve B), the absorption peak at 1740 cm^{-1} was the stretching vibration of carbonyl group in the ester bond. Simultaneously, the characteristic peaks of hydroxyl groups in cholesterol at 3435 cm^{-1} disappeared (Fig. 3, curve A). Second step, Chol-NH_2 (Fig. 3, curve C) was synthesized via an aminolysis reaction between the cholesterol ester and butanediamine. 1700 cm^{-1} was the characteristic peak of amideI, which was the stretching vibration of carbonyl group. 1602 cm^{-1} was the characteristic peak of amideII, which was the in plane flexural vibration of –NH–. ^{1}H NMR analysis of Chol-NH_2 (Fig. 2B) showed the signals at 3.25 ppm was characteristic absorption of –$NHCH_2$-. Third step, the carboxyl group of HA was bound to the amino group of Chol-NH_2 via acylation reaction. In FTIR of Chol-HA (Fig. 3, curve E), 1057,

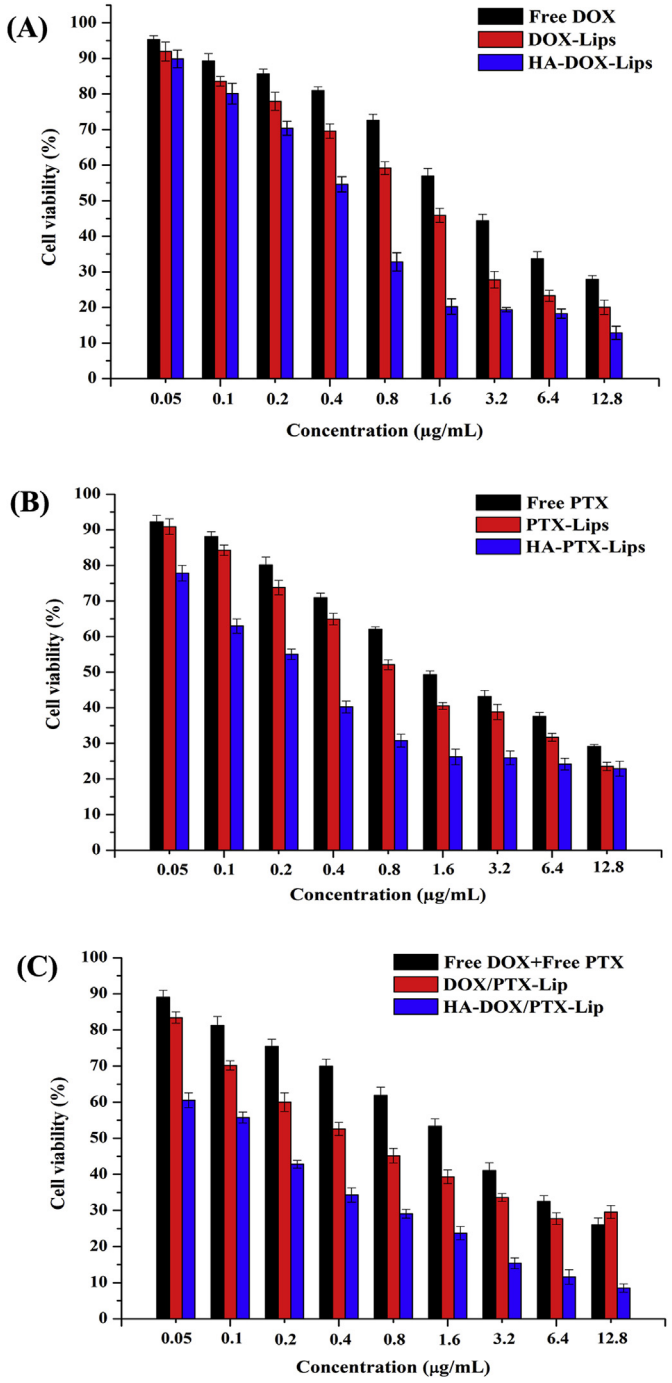

Fig. 11. The cytotoxicity study of free DOX, DOX-Lip and HA-DOX-Lip (A) in MCF-7 cells; free PTX, PTX-Lip and HA-PTX-Lip (B) in MCF-7 cells; free drug combination and dual drug loaded HA-modified and non-modified liposomes in MCF-7 cells for 48 h (mean ± SD, n = 6).

1086, 1189 cm^{-1} were characteristic absorption of sugar unit, and the telescopic vibration of –CH– at 2930 cm^{-1} was stronger than that in HA (Fig. 3, curve D). As shown in Fig. 2D, the *N*-acetyl group in the sugar unit of HA was observed at 2.10 ppm (-$NHCOCH_3$). In summary, Chol-HA conjugate was successfully synthesized.

The DS of cholesterol in Chol-HA conjugate was calculated by the integration ratio between the characteristic peaks of methine group in cholesterol at 5.35 ppm and the N-acetyl group in HA at 1.8 ppm in the ^1H NMR of Chol-HA conjugate. When the molar ratio of cholesterol to HA was 1:1, the DS of cholesterol in Chol-HA conjugate was 7.22%.

Blood compatibility evaluation is a work that must be carried out before the clinical application of biomaterials in direct contact with blood. The hemolysis assay is a widely acknowledged and sensitive acute toxicity screening test. Hemolysis of Chol-HA conjugate with different concentrations was compared with 2% TritonX-100, a non-ionic surfactant that is considered as 100% hemolysis. According to the American Society for Testing and Materials (ASTM F756-00, 2000), biomaterials can be classified as follows based on the degree of hemolysis: non-hemolytic (0–2% hemolysis), slightly hemolytic (2–5% hemolysis), and hemolytic (> 5% hemolysis) [42]. As shown in Table 1, compared with the positive control (2% TritonX-100), the hemolysis rate of Chol-HA conjugate was lower. With the increase of copolymer concentration, the hemolysis rate also increased from 0.79 to 3.59%, they revealed less than 5% hemolysis rate at a concentration of 2 mg/mL, which indicate that the Chol-HA conjugater has good blood compatibility and could be safe for *in vivo* application.

Table 3
IC_{50} and CI_{50} of different formulations against MCF-7 cells for 48 h incubation time.

Samples	IC_{50} (μg/mL)	CI_{50}
Free DOX	2.14	/
Free PTX	0.81	/
Free D + Free P	1.25/0.48	1.18
DOX-Lip	1.29	
PTX-Lip	0.92	
DOX/PTX-Lip	0.51/0.20	0.62
HA-D-Lip	0.59	/
HA-P-Lip	0.31	/
HA-D/P-Lip	0.14/0.06	0.43

The following expressions in this table are the same meaning.
[a] The IC_{50} values of "1.25/0.48" means that the IC_{50} values of DOX and PTX in the combination of "Free D + Free P" is 1.25 μg/mL and 0.48 μg/mL, respectively.

3.2. Characterization of liposomes

HA was inserted into the bilayer of liposome by post-insertion method in this study. The particle size, PDI, Zeta potential and encapsulation efficiency were listed in Table 2. The results showed that the size of all formulations we prepared in this study were about in the range of 90–130 nm and had PDI of less than 0.25. Previous study have shown that a smaller particle size (< 200 nm), below the pore size of leaky vasculatures, along with poor lymphatic drainage, provides a suitable condition for the aggregation and localization of nanoparticles in the solid tumor site [43,44]. Small nanoparticles (size about 100 nm) with a specific structure (for example, PEGylated liposomes) have stronger ability than large nanoparticles to avoid the phagocytosis of RES, because of the high density of PEG on the surface of particles [53]. Moreover, due to the carboxyl group of HA molecules on the surface of HA-modified liposomes, the surface charge of liposomes changed from positive to negative, and the particle size increased in comparison to non-modified liposomes, which indicated that HA has successfully covered the outer surface of liposome. Hydrophilic HA is an alternative candidate for PEG molecules in long-circulating liposomes. Compared with non-modified liposome, HA-modified liposome could avoid the phagocytosis of the RES and prolong the blood circulation time. The encapsulation efficiency of DOX and PTX were about 93.6% and 70.4% in HA-D/P-Lip, respectively. Transmission electron microscope (TEM) was used to observe the morphology of liposomes. As shown in Fig. 4C and D, TEM image revealed that HA-D/P-Lip and HA-Lip were spherical in shape with uniform size distribution, and there was no aggregation between particles.

The hyaluronic acid on Chol-HA was hydrolyzed to monosaccharide containing uronic acid structure under the action of concentrated sulfuric acid. Uronic acid reacted with carbazole to form purplish red complex with UV absorption at 530 nm wavelength. The content of

Chol-HA was calculated according to the calibration curve. In this experiment, the content of Chol-HA in HA-lip calculated by carbazole method is 9.5% mol of total lipids.

3.3. Stability study

Particle size, as one of the most important parameters, was often used to explore the stability of nanoparticles. Nanoparticle stability under physiological conditions is a prerequisite for their application *in vivo* [44]. As shown in Fig. 5, the particle size of HA-D/P-Lip in 50% FBS and pH 7.4 PBS did not display a sharp increase or decrease over 48 h, indicating that the liposomes were stable in different conditions *in vitro*, while D/P-Lip was unstable within 48 h, especially in serum. This could be due to the presence of hydrophilic hyaluronic acid, which forms a protective barrier in the outer layer of liposome. This stereospecific blockade could avoid the accumulation of liposomes and attenuating the recognition and destruction of liposomes by plasma components, thus making the liposomes more stable [25].

3.4. In vitro drug release

In vitro drug release study was performed to examine the drug release properties of liposomes under different pH conditions. The release profiles of DOX and PTX from HA-D/P-Lip and D/P-Lip were represented in Fig. 6. As shown in Fig. 6A, compared with DOX solution, all liposomal formulations exhibited sustained release process, and no burst release was observed. Nearly 50% of DOX was released from D/P-Lip over 72 h under pH 7.4, while the cumulative release of DOX in HA-D/P-Lip was only 43%, indicating that the existence of HA reduced the release rate of DOX and PTX from HA-D/P-Lip. This might be due to the existence of HA molecules on liposomes. HA is a kind of strong hydrophilic polymer. When the liposomes are wrapped around by HA, HA molecules expanded in aqueous solution after adsorb water rapidly, forming a dense hydration membrane around the liposomes, which decreases the fluidity and permeability of phospholipid bilayer, thus hindering the drug release [43–45]. The total DOX release of HA-D/P-Lip during 72 h was about 43% under pH 7.4, whereas, the release of DOX in pH 5.5 PBS buffer was up to 90%. This might be due to the instability of liposome structure and drug properties. On the one hand, hyaluronic acid is unstable in acidic solution and easy to hydrolyze, resulting in the random scission of its polymer chains. Eventually, the structure of liposomes is no longer complete [46,47]. On the other hand, the increase of DOX solubility in acidic environment and the weakening of interaction between DOX and liposomal bilayers [48]. We speculated that another possibility is that when the HA is hydrolyzed, the lipid bilayer was exposed, but the cholesterol segment in Chol-HA conjugate is still in the bilayers, and excessive cholesterol is unfavorable to the stability of the bilayers. Therefore, after the protection of the hydrophilic layer was lost, the fluidity and permeability of the phospholipid bilayer increased, and the drug was released from liposome. In addition, a slight delay was observed in the release of PTX (Fig. 6B) compared with DOX, this might be stemmed from solubility difference between PTX with DOX in aqueous solution.

3.5. In vitro cellular uptake

3.5.1. Confocal laser scanning microscopy (CLSM)

CLSM is a very important equipment to obtain the information about the intracellular transport and localization of nanoparticles. The *in vitro* cellular uptake of HA-DOX-Lip in comparison to free DOX and DOX-Lip were detected in MCF-7 cells (relatively high CD44 expression) and HepG2 cells (relatively low CD44 expression) after 2 and 4 h incubation. As shown in Fig. 7, red and blue fluorescence signals correspond to DOX and DAPI (nuclei dye), respectively. The obvious red signals were mainly accumulated in the nuclear region and a few in the cytoplasm in both cells, indicating that liposomal formulation was initially taken up into cells, DOX molecule was gradually released from liposomes and entered into nuclei by simple diffusion. Fig. 7A and C showed fluorescence intensity of HA-DOX-Lip in MCF-7 cells was stronger than D-Lip and free DOX. However, fluorescence intensity of HA-DOX-Lip in HepG2 cells was weaker in comparison to MCF-7 cells. The possible explanation for this results is that the different transmembrane transport mechanism of free DOX, DOX-Lip and HA-DOX-Lip.

For free drugs, doxorubicin is water-soluble compound, and enter into cells via faster passive diffusion [21]. When the DOX concentrations in and outside the cell membrane are identical, diffusion process would not transmit more DOX into cells. Another important cause decreasing the cellular uptake of free DOX is drug efflux. Drugs are quickly identified and excreted out of the cells when the drug enters into cells [43]. DOX-Lip penetrates into cells via passive targeting and endocytosis. HA-DOX-Lip enters into cells via active targeting and endocytosis. CD44 receptors are the specific glycoprotein that overexpressed on some tumor cell membrane, and its specific ligand is hyaluronic acid. Because the expression of CD44 receptor in MCF-7 cells is higher than that in HepG2 cells, the CD44-mediated endocytosis is more obvious [33]. As explained by the above results, HA-DOX-Lip has superior capacity of penetrate into MCF-7 cells, this is owing to the specific affinity between HA and CD44, which led to receptor-ligand-mediated endocytosis (active targeting). Previous studies demonstrated that CD44-mediated endocytosis is a probable mechanism for internalization of any HA-targeted nanocarriers [49].

3.5.2. Flow cytometry (FCM)

Flow cytometry analysis was used to measure the *in vitro* cellular uptake quantitatively. Fig. 8 showed the mean fluorescence intensity of free DOX, DOX-Lip and HA-DOX-Lip in MCF-7 cells and HepG2 cells with the DOX concentration was 10 μg/mL. As described in Fig. 8, the fluorescence intensity in cells gradually increased with the extension of incubation time. For MCF-7 cells, the fluorescence intensity of HA-DOX-Lip reached the maximum value when incubated for 4 h, and for HepG2 cells, the fluorescence intensity of HA-DOX-Lip was lower than that of free DOX group at the same time. The uptake of HA-DOX-Lip in MCF-7 cell group exhibited remarkably higher uptake level than HepG2 cell group due to the differences in the amount of receptor expression, and all the above results are consistent with CLSM analysis, which might be the effect of endocytosis mechanism.

3.6. Cellular uptake mechanism of HA-DOX-lip

In order to detect the possible endocytosis pathway of HA-DOX-Lip on MCF-7 cells, several endocytosis inhibitors were used in this study, and the cells treated without any inhibitors was set as control group. As shown in Fig. 9, the uptake of HA-DOX-Lip by MCF-7 cells decreased to 23% ($p < 0.001$) at 4 °C, which may be due to the lower temperature that led to slower metabolic activity of cells, indicating that the cellular uptake of MCF-7 cells was in a temperature-dependent manner. No changes in the uptake of HA-DOX-Lip were observed after incubation with a macropinocytosis inhibitor of amiloride [50]. Chlorpromazine, cyclodextrin and sodium azide were able to inhibit the uptake (down to 79%, 83% and 81%, respectively), indicating that clathrin-mediated endocytosis, caveolae-dependent endocytosis and energy-dependent endocytosis were probably involved in the uptake behavior [50]. Cellular uptake of HA-DOX-Lip was remarkably decreased after incubation with free HA ($p < 0.001$), which suggested receptor-mediated endocytosis was involved in the pathways. Accordingly, the uptake mechanism of HA-DOX-Lip were energy-, caveolae-dependent endocytosis, clathrin-mediated endocytosis and receptor-mediated endocytosis.

3.7. In vitro cytotoxicity

The biocompatibility of HA-Lip was evaluated by MTT assay in

MCF-7 cells (human breast cancer cell), HepG2 cells (human hepatoma cells) and L929 cells (mouse fibroblast cell). As shown in Fig. 10, after 48 h of exposure, blank liposome (HA-Lip) showed lower cytotoxicity effect in all cell lines, and the cell survival rate was above 85%, indicating that HA-Lip had better safety and biocompatibility.

The cytotoxicity of free drugs and drug-loaded liposomes was measured toward MCF-7 cells with the help of MTT assay. The dose-response curves are represented in Fig. 11, all experimental groups had dose-dependent characteristic, and both HA-DOX-Lip and HA-PTX-Lip exhibited superior cytotoxicity *in vitro* in comparison to free drugs and non-modified drug-loaded liposomes after incubation for 48 h. Compared with single drug treatment, dual-drug combination appliance has better cytotoxicity (Fig. 11C). The IC_{50} values of free drugs and drug-loaded liposomes and combination index (CI_{50}) values were summarized in Table 3. The IC_{50} values of HA-DOX-Lip and HA-PTX-Lip were lower than that of free single drug or non-modified single drug-loaded liposomes, respectively. This might be due to the different uptake pathways in free drug and liposomes and drug resistance, and also involves the controlled release of liposomes [6]. Bare drug molecules penetrate into cells via passive diffusion, HA-DOX-Lip or HA-PTX-Lip had high affinity to CD44 receptor and resulted in active targeting (CD44-mediated endocytosis). The above results concluded that the active targeting of HA-DOX-Lip or HA-PTX-Lip by CD44-mediated endocytosis lead to more drug molecules delivered into cells and higher cytotoxicity. These results were consistent with the results of Fatemeh et al. [43]. The CI_{50} values lower than 1, equal to 1, or higher than 1 indicated synergistic effect, additive effect, or antagonistic effect, respectively. The CI_{50} value of Free DOX + Free PTX was 1.18, suggested that the combination of free DOX + free PTX did not exhibit synergistic effect, while the DOX/PTX-Lip group and HA-DOX/PTX-Lip group showed synergistic effect, indicating that co-delivery of DOX and PTX in a same carrier had evident superiority as compared with free drug combination.

4. Conclusions

In this study, Chol-HA conjugate were successfully synthesized, and Hyaluronic acid modified liposomal drug delivery system which co-loaded DOX and PTX was successfully developed. The liposomal formulations have suitable particle size of about 120 nm, with a negative surface charge. *In vitro*, HA-D/P-Lip has good stability, exhibited enhanced cytotoxicity than free drugs, and improved cellular uptake level based on EPR effect and CD44-mediated endocytosis between HA and CD44. Besides, dual-drug combination strategies showed high anti-tumor effect than single drug treatment. Hence, the liposomal delivery system we prepared in this study could be a promising nanocarrier for targeted tumor therapy.

Conflicts of interest

None.

Acknowledgments

This work was financially supported by the National Natural Science Foundation of China (81703717) and the Shandong Provincial Natural Science Foundation (ZR2014HQ096).

References

[1] F. Danhier, O. Feron, V. Préat, To exploit the tumor microenvironment: passive and active tumor targeting of nanocarriers for anti-cancer drug delivery, J. Control. Release 148 (2010) 135–146.
[2] M.-H. Chen, Y. Zhang, Z.-J. Chen, S.-Z. Xie, X.-M. Luo, X.-H. Li, Synergistic anti-tumor efficacy of redox and pH dually responsive micelleplexes for co-delivery of camptothecin and genes, Acta Biomater. 49 (2017) 444–455.
[3] O. Tacar, P. Sriamornsakb, C. Dass, Doxorubicin: an update on anticancer molecular action, toxicity and novel drug delivery systems, J. Pharm. Pharmacol. 65 (2013) 157–170.
[4] Y. Pommier, E. Leo, H.-L. Zhang, C. Marchand, DNA topoisomerases and their poisoning by anticancer and antibacterial drugs, Chem. Biol. 17 (2010) 421–433.
[5] M.-H. Xiong, L.-Y. Tang, J. Wang, Synthesis and properties of diblock copolymers of poly (ethylene glycol) and poly (2-methoxyethyl ethylene phosphate) for enhanced paclitaxel solubility, Acta Polym. Sin. (2011) 853–860.
[6] S.-X. Lv, Z.-H. Tang, M.-Q. Li, J. Lin, W.-T. Song, H.-Y. Liu, Y.-B. Huang, Y.-Y. Zhang, X.-S. Chen, Co-delivery of doxorubicin and paclitaxel by PEG-polypeptide nanovehicle for the treatment of non-small cell lung cancer, Biomaterials 35 (2014) 6118–6129.
[7] T. Shigehiro, M. kasai, S. Murakami, Efficient drug delivery of paclitaxel glycoside: a novel solubility gradient encapsulation into liposomes coupled with immunoliposomes preparation, PLoS One 9 (2014) e107976.
[8] R. He, C.-H. Yin, Trimethyl chitosan based conjugates for oral and intravenous delivery of paclitaxel, Acta Biomater. 53 (2017) 355–366.
[9] X.-L. Xu, X.-S. Chen, Z.-F. Wang, X.-B. Jing, Ultrafine PEG-PLA fibers loaded with both paclitaxel and doxorubicin hydrochloride and their in vitro cytotoxicity, Eur. J. Pharm. Biopharm. 72 (2009) 18–25.
[10] H. Gogas, C. Papadimitriou, H. Kalofonos, D. Bafaloukos, G. Fountzilas, D. Tsavdaridis, A. Anagnostopoulos, A. Onyenadum, P. Papakostas, T. Economopoulos, C. Christodoulou, P. Kosmidis, C. Markopoulos, Neoadjuvant chemotherapy with a combination of pegylated liposomal doxorubicin (Caelyx®) and paclitaxel in locally advanced breast cancer: a phase II study by the Hellenic Cooperative Oncology Group, Ann. Oncol. 13 (2012) 1737–1742.
[11] D.-J. Zhao, J.-L. Wu, C.-X. Li, H.-Y. Zhang, Z.-H. Li, Y.-X. Luan, Precise ratiometric loading of PTX and DOX based on redox-sensitive mixed micelles for cancer therapy, Colloids Surfaces B Biointerfaces 155 (2017) 1551–1560.
[12] F. Greco, M. Vicent, Combination therapy: opportunities and challenges for polymer-drug conjugates as anticancer nanomedicines, Adv. Drug Deliv. Rev. 61 (2009) 1203–1213.
[13] P. Zhang, J. Li, M. Ghazwani, W.-C. Zhao, Y.-X. Huang, X.-L. Zhang, R. Venkataramanan, L. Song, Effective co-delivery of doxorubicin and dasatinib using a PEG-Fmoc nanocarrier for combination cancer chemotherapy, Biomaterials 67 (2015) 104–114.
[14] M.-Q. Yuan, Y. Qiu, L. Zhang, H.-L. Gao, Q. He, Targeted delivery of transferrin and TAT co-modified liposomes encapsulating both paclitaxel and doxorubicin for melanoma, Drug Deliv. 23 (2016) 1171–1183.
[15] S.-X. Lv, Z.-H. Tang, M.-Q. Li, J. Lin, W.-T. Song, H.-Y. Liu, Y.-B. Huang, Y.-Y. Zhang, X.-S. Chen, Co-delivery of doxorubicin and paclitaxel by PEG-polypeptide nanovehicle for the treatment of non-small cell lung cancer, Biomaterials 11 (2014) 1–12.
[16] F. Ahmed, R. Pakunlu, A. Brannan, F. Bates, T. Minko, D. Discher, Biodegradable polymersomes loaded with both paclitaxel and doxorubicin permeate and shrink tumors, inducing apoptosis in proportion to accumulated drug, J. Control. Release 116 (2006) 150e8.
[17] H. Wang, Y. Zhao, Y. Wu, Y.-L. Hu, K.-H. Nan, G.-J. Nie, H. Chen, Enhanced anti-tumor efficacy by co-delivery of doxorubicin and paclitaxel with amphiphilic methoxy PEG-PLGA copolymer nanoparticles, Biomaterials 32 (2011) 8281–8290.
[18] E. Gullotti, Y. Yeo, Extracellularly activated nanocarriers: a new paradigm of tumor targeted drug delivery, Mol. Pharm. 6 (2009) 1041–1051.
[19] A. Wojcicki, H. Hillaireau, T. Nascimento, S. Arpicco, M. Taverna, S. Ribes, M. Bourge, V. Nicolas, A. Bochot, C. Vauthier, N. Tsapis, E. Fattal, Hyaluronic acid-bearing lipoplexes: physico-chemical characterization and in vitro targeting of the CD44 receptor, J. Control. Release 162 (2012) 545–552.
[20] F. Sauvage, S. Franzè, A. Bruneau, M. Alami, S. Denis, V. Nicolas, S. Lesieur, F. Legrand, G. Barratt, S. Messaoudi, J. Gauduchon, Formulation and in vitro efficacy of liposomes containing the Hsp90 inhibitor 6BrCaQ in prostate cancer cells, Int. J. Pharm. 499 (2016) 101–109.
[21] S.-L. Zhou, T. Zhang, B. Peng, X. Luo, X.-R. Liu, L. Hu, Y. Liu, D.-H. Di, Y.-Z. Song, Y.-H. Deng, Targeted delivery of epirubicin to tumor-associated macrophages by sialic acid-cholesterol conjugate modified liposomes with improved antitumor activity, Int. J. Pharm. 523 (2017) 203–216.
[22] B. Haley, E. Frenkel, Nanoparticles for drug delivery in cancer treatment, Urol. Oncol. 26 (2008) 57–64.
[23] S. Tanaka, M. Shiramoto, Y. Miyashita, Y. Fujishima, Tumor targeting based on the effect of enhanced permeability and retention (EPR) and the mechanism of receptor mediated endocytosis (RME), Int. J. Pharm. 227 (2004) 39–61.
[24] P. Sapra, P. Tyagi, T. Allen, Ligand-targeted liposomes for cancer treatment, Cur, Drug Deliv. 2 (2005) 369–381.
[25] D. Peer, R. Margalit, Tumor-targeted hyaluronan nanoliposomes increase the anti-tumor activity of liposomal doxorubicin in syngeneic and human Xenograft mouse tumor models, Neoplasia 6 (2004) 343–353.
[26] A. Blum, J. Kammeyer, A. Rush, C. Callmann, C. Hahn, N. Gianneschi, Stimuli-responsive nanomaterials for biomedical applications, J. Am. Chem. Soc. 137 (2015) 2140–2154.
[27] C. Gong, M. Shan, B. Li, G. Wu, A pH and redox dual stimuli-responsive poly(amino acid) derivative for controlled drug release, Colloids Surfaces B Biointerfaces 146 (2016) 396–405.
[28] Y. Di, T. Li, Z.-H. Zhu, F. Chen, L.-Q. Jia, W.-B. Liu, X.-M. Gai, Y.-Y. Wang, W.-S. Pan, X.-G. Yang, pH-sensitive and folic acid-targeted MPEG-PHIS/FA-PEG-VE mixed micelles for the delivery of PTX-VE and their antitumor activity, Int. J. Nanomed. 12 (2017) 5863–5877.
[29] L.-L. Wang, B.-C. Tian, J. Zhang, K.-K. Li, Y. Liang, Y.-J. Sun, Y.-Y. Ding, J.-T. Han, Coordinated pH/redox dual-sensitive and hepatoma-targeted multifunctional polymeric micelle system for stimuli-triggered doxorubicin release: synthesis,

characterization and in vitro evaluation, Int. J. Pharm. 501 (2016) 221–235.
[30] X.-L. Hu, S. Liu, Y.-B. Huang, X.-S. Chen, X.-B. Jing, Biodegradable block copolymer-doxorubicin conjugates via different linkages: preparation, characterization, and in vitro evaluation, Biomacromolecules 11 (2010) 2094–2102.
[31] N. Song, W.-M. Liu, Q. Tu, R. Liu, Y.-R. Zhang, J.-Y. Wang, Preparation and in vitro properties of redox-responsive polymeric nanoparticles for paclitaxel delivery, Colloids Surfaces B Biointerfaces 87 (2011) 454–463.
[32] W.-H. Pan, M.-Y. Qin, G.-G. Zhang, Y.-M. Long, W.-Y. Ruan, J.-T. Pan, Z.-S. Wu, T. Wan, C.-B. Wu, Y.-H. Xu, Combination of hydrotropic nicotinamide with nanoparticles for enhancing tacrolimus percutaneous delivery, Int. J. Nanomed. 11 (2016) 4037–4050.
[33] J.-L. Wang, W.-Z. Ma, Q. Guo, Y. Li, Z.-D. Hu, Z.-X. Zhu, X.-H. Wang, Y.-F. Zhao, X.-Y. Chai, P.-F. Tu, The effect of dual-functional hyaluronic acid-vitamin E succinate micelle on targeting delivery of doxorubicin, Int. J. Nanomed. 11 (2016) 5851–5870.
[34] L.-J. Zhang, H. Cao, J.-X. Zhang, C.-L. Yang, T.-T. Hu, H.-L. Li, W. Yang, G. He, X.-R. Song, A.-P. Tong, G. Guo, R. Li, Y. Jiang, J.-Y. Liu, L. Cai, Y. Zheng, Comparative study of (Asp)7-CHOL-modified liposome prepared using pre-insertion and post-insertion methods for bone targeting in vivo, J. Drug Target. 25 (2017) 149–155.
[35] Y.-Y. Chi, X.-L. Yin, K.-X. Sun, S.-S. Feng, J.-H. Liu, D.-Q. Chen, C.-Y. Guo, Z.-M. Wu, Redox-sensitive and hyaluronic acid functionalized liposomes for cytoplasmic drug delivery to osteosarcoma in animal models, J. Control. Release 261 (2017) 113–125.
[36] X.-M. Li, L.-Y. Ding, Y.-L. Xu, Y.-L. Wang, Q.-N. Ping, Targeted delivery of doxorubicin using stealth liposomes modified with transferrin, Int. J. Pharm. 373 (2009) 116–123.
[37] J. Sun, Y.-Z. Song, M. Lu, X.-Y. Lin, Y. Liu, S.-L. Zhou, Y.-Q. Su, Y.-H. Deng, Evaluation of the antitumor effect of dexamethasone palmitate and doxorubicin co-loaded liposomes modified with a sialic acid- octadecylamine conjugate, Eur. J. Pharm. Sci. 93 (2016) 177–183.
[38] H. Zhao, M. Wang, S. Yu, Paclitaxel-loaded, folic-acid-targeted and TAT-peptide-conjugated polymeric liposomes: in vitro and in vivo evaluation, Pharm. Res. 27 (2010) 1914–1926.
[39] N. Oueslatia, P. Leblanca, C. Schiavoa, E. Rondagsa, S. Meunier, R. Kapel, I. Marc, CTAB turbidimetric method for assaying hyaluronic acid in complex environments and under cross-linked form, Carbohydr. Polym. 112 (2014) 102–108.
[40] M. Kosakai, Z. Yosizawa, A partial modification of the carbazole method of bitter and muir for quantitation of hexuronic acids, Anal. Biochem. 93 (1979) 295–298.
[41] C. Surace, S. Arpicco, A. Wojcicki, V. Marsaud, C. Bouclier, D. Clay, L. Cattel, J. Renoir, E. Fattal, Lipoplexes targeting the CD44 hyaluronic acid receptor for efficient transfection of breast cancer cells, Mol. Pharm. 6 (2009) 1062–1073.
[42] Z.-L. He, Z. Shi, W. Sun, J. Ma, J. Xia, X. Zhang, W. Chen, J. Huang, Hemocompatibility of folic-acid-conjugated amphiphilic PEG-PLGA copolymer nanoparticles for co-delivery of cisplatin and paclitaxel: treatment effects for non-small-cell lung cancer, Tumor Biol. 37 (2016) 7809–7821.
[43] F. Ravar, E. Saadat, M. Gholami, P. Dehghankelishadi, M. Mahdavi, S. Azami, A. Farid, Hyaluronic acid-coated liposomes for targeted delivery of paclitaxel, in-vitro characterization and in-vivo evaluation, J. Control. Release 229 (2016) 10–22.
[44] Tao Yang, Min-Koo Choi, Fu-De Cui, Jung Sun Kim, Suk-Jae Chung, Chang-Koo Shim, Dae-Duk Kim, Preparation and evaluation of paclitaxel-loaded PEGylated immunoliposome, J. Control. Release 120 (2007) 169–177.
[45] D.A. Ossipov, Nanostructured hyaluronic acid-based materials for active delivery to cancer, Expert Opin. Drug Deliv. 7 (6) (2010) 681–703.
[46] E.-J. Kim, J. Yang, J. Park, S. Kim, H.-K. Nam, I.-Y. Jong, J.-S. Suh, S. Haam, Y.-M. Huh, Consecutive targetable smart nanoprobe for molecular recognition of cytoplasmic microRNA in metastatic breast cancer, ACS Nano 6 (2012) 8525–8535.
[47] T.-L. Nascimento, H. Hillaireau, J. Vergnaud, E. Fattal, Lipid-based nanosystems for CD44 targeting in cancer treatment: recent significant advances, ongoing challenges and unmet needs, Nanomedicine 11 (2016) 1865–1887.
[48] J.-H. Park, H.-J. Cho, H.-Y. Yoon, I.-S. Yoon, S.-H. Ko, J.-S. Shim, J.-H. Cho, J.-H. Park, K. Kim, I.-C. Kwon, D.-D. Kim, Hyaluronic acid derivative-coated nanohybrid liposomes for cancer imaging and drug delivery, J. Control. Release 174 (2014) 98–108.
[49] Z.-H. Xu, W.-W. Gu, J. Huang, H. Sui, Z.-H. Zhou, Y.-X. Yang, Z. Yan, Y.-P. Li, In vitro and in vivo evaluation of actively targetable nanoparticles for paclitaxel delivery, Int. J. Pharm. 288 (2005) 361–368.
[50] Q.-Y. Zhang, J. Tang, L. Fu, R. Ran, Y.-Y. Liu, M.-Q. Yuan, Q. He, A pH-responsive α-helical cell penetrating peptide-mediated liposomal delivery system, Biomaterials 34 (2013) 7980–7993.
[51] E. Saadat, M. Amini, M.R. Khoshayand, R. Dinarvand, F.A. Dorkoosh, Synthesis and optimization of a novel polymeric micelle based on hyaluronic acid and phospholipids for delivery of paclitaxel, in vitro and in-vivo evaluation, Int. J. Pharm. 475 (2014) 163–173.
[52] T. Chou, Theoretical basis, experimental design, and computerized simulation of synergism and antagonism in drug combination studies, Pharmacol. Rev. 58 (2006) 621–681.
[53] F. Yuan, M. Dellina, D. Fukumura, M. Leunig, D.-A. Berk, R.-K. Jain, Vascular permeability in a human tumor xenograft: molecular size dependence and cutoff size, Cancer Res. 55 (1995) 3752–3756.